High-pressure magnetic susceptibility experiments on the heavy lanthanides Gd, Tb, Dy, Ho, Er, and Tm

D. D. Jackson,* V. Malba, and S. T. Weir
Lawrence Livermore National Laboratory, Livermore, California 94551, USA

P. A. Baker and Y. K. Vohra
University of Alabama at Birmingham, Birmingham, Alabama 35124, USA
(Received 19 November 2004; published 26 May 2005)

The high-pressure magnetic properties of the heavy lanthanide elements Gd, Tb, Dy, Ho, Er, and Tm have been investigated using ac-magnetic susceptibility with a diamond anvil cell. It is found that the magnetic transition temperatures monotonically decrease with increasing pressure. In addition, the amplitudes of the magnetic transition signals decrease with increasing pressure, with the signals all eventually disappearing at pressures of 20 GPa. In contrast to previous studies, we see no evidence of any pressure-induced transitions from one magnetically ordered phase to another in Gd, Tb, Dy, or Ho. The transition temperatures T_{crit} are all found to drop at a rate proportional to their de Gennes factor, and the values of $T_{crit}/T_{crit}(P=0)$ vs P/P_{crit}, where P_{crit} is the pressure at which the magnetic transition disappears, all sit on a single phase diagram.

DOI: 10.1103/PhysRevB.71.184416 PACS number(s): 75.30.−m, 74.62.Fj, 75.50.−y

I. INTRODUCTION

The heavy lanthanide elements exhibit a wide variety of magnetic ordering at low temperatures due to an interplay between strong correlation effects and indirect exchange effects involving their f electrons.[1,2] The very compact nature of the lanthanide $4f$ shells gives rise to strong intra-atomic f electron correlations and to the effective Mott-localization of the $4f$ electrons, resulting in the formation of localized magnetic moments at the ionic sites. Due to a Ruderman-Kittel-Kasuya-Yosida (RKKY) indirect-exchange mechanism, in which an effective interionic f-spin-to-f-spin interaction is mediated by the surrounding Fermi sea of conduction electrons, magnetic ordering is exhibited in the heavy lanthanides Gd, Tb, Dy, Ho, Er, and Tm at low temperatures.

The RKKY interaction, which couples the f electron spins, is long ranged and oscillatory, and so the magnetic moment at any ionic site is influenced by a large number of aligning fields from surrounding ions. This results in the rich variety of possible magnetically ordered phases exhibited by the lanthanides. The application of high pressures changes the interatomic distances and can alter the net balance of the aligning fields felt by the magnetic moments. High pressure can also produce changes in the density of states, which has an effect on the band structure of the conduction electrons. Through high pressure magnetic susceptibility experiments, we can examine how these changes affect the magnetic ordering temperatures of the heavy lanthanides and explore the possibility of pressure-induced magnetic transitions.

Magnetic susceptibility experiments on the heavy lanthanides under pressure have been previously performed by several groups.[3–13] McWhan and Stevens[6] studied Gd, Tb, Dy, and Ho and saw evidence of magnetic phase transitions in these elements, detected by the appearance of peaks in the ac-magnetic susceptibility at high pressures. Their results for the magnetic susceptibility of Gd showed complicated behavior which included up to four peaks at high pressures, whereas at other pressures only one or two peaks were observed. They cautioned, however, that the observed transitions were sluggish and that it was difficult to unambiguously assign peaks to low-pressure versus high-pressure phases or to even be sure if the peaks represent equilibrium conditions. Iwamoto *et al.*,[12] on the other hand, did not observe any signs of multiple susceptibility peaks in their high pressure gadolinium experiments, and they suggested that the multiple peaks may have been due to uniaxial stress conditions or large pressure gradients in the experiments by McWhan and Stevens.

We report here on high pressure ac-magnetic susceptibility experiments performed on six heavy lanthanide elements: Gd, Tb, Dy, Ho, Er, and Tm. The purpose of these experiments was to investigate the pressure dependencies of the ferromagnetic (FM) and antiferromagnetic (AFM) transitions of these elements and to see whether they exhibit magnetic phase transitions of the type reported in previous studies.

II. EXPERIMENTAL TECHNIQUE

We performed ac-magnetic susceptibility experiments as a function of both pressure and temperature using a nonmagnetic Be−Cu diamond anvil cell (model SR-DAC-KY03-1 from Kyowa Seisakusho) and a closed cycle He refrigerator (Cryomech ST-15). The sample pressure was determined by the ruby fluorescence technique,[14–16] while the diamond anvil cell (DAC) was cooled *in situ*. This allows us to correct for any small pressure changes due to the thermal contraction of the DAC.

To detect changes in the magnetic susceptibility of the high-pressure sample, we subjected the sample to a small ac-magnetic field (typically 3 Oe @ 10 kHz) while monitoring the voltage induced in a tiny sensing coil located near the sample. The ac-magnetic field was generated by a 40-turn excitation coil of 32 AWG (0.2019 mm diameter) manganin

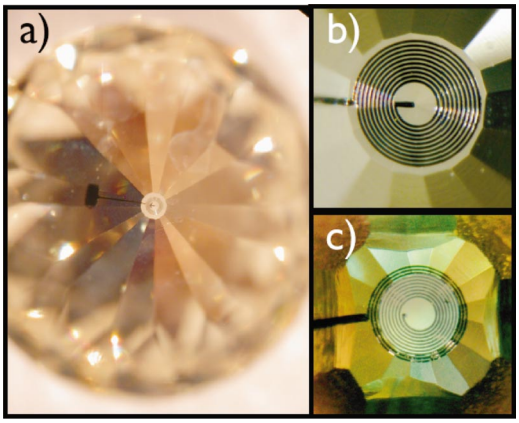

FIG. 1. (Color) A designer diamond anvil with a ten-turn magnetic sensing coil. The thin-film tungsten coil has an outer diameter of 280 μm, an inner diameter of 90 μm, and a linewidth of 5 μm. (a) A photograph of the entire diamond anvil, showing both the sensing coil and an electrical connection pad on the side of the anvil. (b) A magnified view of the culet showing the sensing coil in more detail. (c) The culet after being encased in a layer of diamond approximately 10 μm thick.

wire wrapped around the base of one of the diamond anvils. The rms current through the excitation coil was typically about 90 mA. The sensing coil was a 10-turn, thin-film coil of tungsten that was fabricated onto a diamond anvil culet and then encapsulated in a thin film of diamond (Fig. 1). This allowed us to locate the sensing coil just a few tens of microns from the sample and obtain an excellent signal-to-background ratio. The outer diameter of the sensing coil was 280 μm, and the inner diameter was 90 μm. A full description of our anvil fabrication process and magnetic susceptibility technique has been previously described elsewhere.[17–19]

The Gd, Tb, Dy, Ho, and Er samples were all greater than 99.9% purity and were in the form of 40-mesh flakes (Alfa Æsar); Tm was cut from a boule from Ames Laboratory, which was also greater than 99.9% purity. The samples were loaded into gaskets made from a high-strength, nonmagnetic alloy (MP35N), along with a small chip of ruby ($\approx$20 μm) for pressure measurement. The starting sample size was typically 75 μm in diameter and 80 μm thick. No methanol-ethanol pressure medium was used in these experiments because of concerns about sample reactivity. The samples were all loaded using a glovebox filled with nitrogen or argon gas. The sample pressure was usually increased by 1–2 GPa steps, with the magnetic susceptibility signal recorded as a function of temperature from 20 K to 296 K at each pressure step.

III. RESULTS

We performed magnetic susceptibility experiments on the six heavy lanthanide elements Gd–Tm. For each element in which we detected AFM ordering (Dy–Tm), the Néel temperature was taken as the peak in the signal voltage. Each element will be individually discussed, with the cumulation of a magnetic phase diagram shown in Fig. 9, and Table I lists the measured pressure dependencies for each transition.

A. Gadolinium

At zero pressure gadolinium exhibits a FM transition when cooled below its Curie temperature T_C=293 K. Some representative high-pressure magnetic susceptibility spectra are shown in Fig. 2. The paramagnetic-to-ferromagnetic transition temperature was defined by the initial rise in the voltage, and it was clearly observable up to a pressure of 5.6 GPa. However, when the sample was loaded from 5.6 to 7.4 GPa the FM signal suddenly disappeared, only to reappear when the pressure was again decreased below 5.5 GPa. In addition, we measured the magnetic susceptibility of Gd using a methanol:ethanol:water mixture (16:3:1),

TABLE I. Measured pressure dependencies for Gd, Tb, Dy, Ho, Er, and Tm.

Element	dT_C/dP (K/GPa, ±5%)[a]	dT_N/dP (K/GPa±5%)[a]	dT_C/dP (K/GPa) others	dT_N/dP (K/GPa) others
Gd	−14.5		−12.5,[b] −10.6,[c] −17.2[d] −16.3,[e] −14.0,[f] −12.2,[g] −13.8[h]	
Tb	−11		−12.4,[i] −12.4[f]	−10.7,[d] −10,[j] −10.8[e] −10.5,[i] −8.4[f]
Dy	−4.6	−6.7	−8,[j] −12.4,[k] −12.7[f]	−6.6,[d] −4,[j] −6.2[e] −5.0,[k] −4.1[f]
Ho		−4.8		−4.8,[d] −4.8[e]
Er		−3.1	−8[k]	−2.6[k]
Tm		−1.0	No Refs.	No Refs.

[a]This work
[b]From Ref. 3
[c]From Ref. 4
[d]From Ref. 6
[e]From Ref. 8
[f]From Ref. 11
[g]From Ref. 12
[h]From Ref. 13
[i]From Ref. 10
[j]From Ref. 5
[k]From Ref. 9

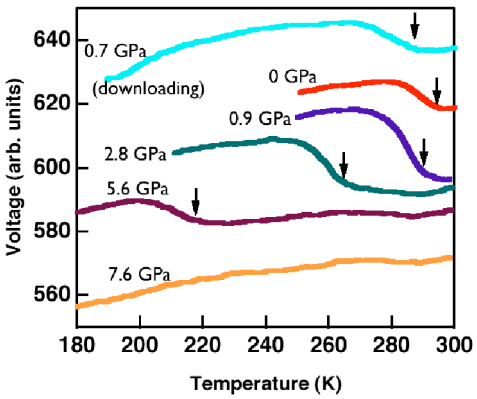

FIG. 2. (Color online) Magnetic susceptibility signal voltage versus temperature taken at various pressures for a gadolinium sample. The arrows show the location of the FM transition.

which produced the same rate of decrease in the Curie temperature versus pressure, while the recovered peak in the signal voltage upon downloading was somewhat larger than it was when no pressure medium was used. The improvements, however, were not large enough to justify the risk of a possible reaction with the pressure medium, so in the following experiments, no pressure medium was used.

At 240 K and ambient pressure, Gd is known to have a ferromagnetic-to-ferromagnetic spin-reorientation transition. This was not observable in our signals, presumably because the difference in the ac susceptibilities of these two FM phases was too small to detect with our system. In addition, we did not observe any of the additional signal peaks reported by McWhan and Stevens in their high-pressure susceptibility experiments on Gd.[6]

B. Terbium

Terbium undergoes an AFM transition (basal-plane spiral structure) at a Néel temperature of T_N=230 K, and then a FM transition at T_C=220 K at zero pressure. Some representative high-pressure spectra are shown in Fig. 3. We clearly observed the FM transition up to a pressure of 6.3 GPa. In

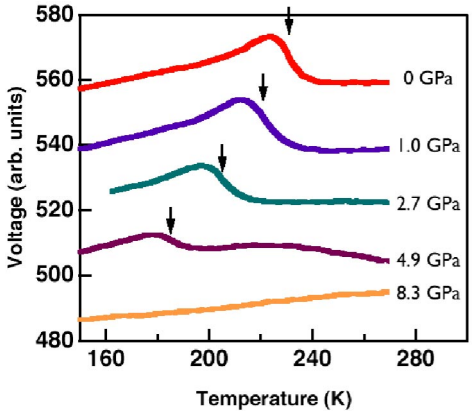

FIG. 3. (Color online) Magnetic susceptibility signal voltage versus temperature taken at various pressures for a terbium sample. The arrows show the location of the FM transition.

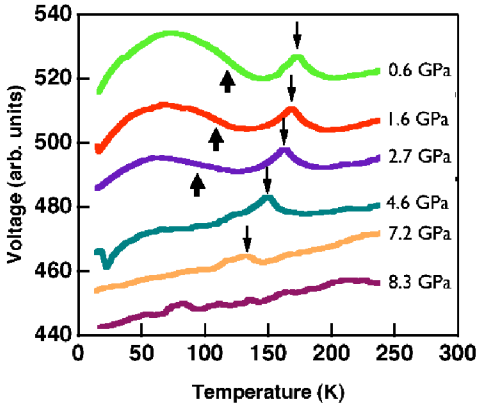

FIG. 4. (Color online) Magnetic susceptibility signal voltage versus temperature taken at various pressures for a dysprosium sample. The arrows pointing up show the location of the FM transition, and the downward arrows show the location of the AFM transition.

this case, because of the different type of FM alignment, the transition temperature was defined by the location of the negative peak in the temperature derivative of the signal voltage, in order to achieve a zero-pressure T_C consistent with the literature value. The AFM transition was either obscured by the nearby FM transition, or its signal was too small for us to detect. At 8.3 GPa, no magnetic transition was observable.

C. Dysprosium

Dysprosium also undergoes both an AFM (basal-plane spiral structure) and a FM transition at low temperatures, with a T_N=176 K and a T_C=87 K. Some high-pressure spectra are shown in Fig. 4. The AFM transition was marked by a small, sharp peak in the signal, and the FM transition was again determined by the location of the negative peak in $d\chi/dT$. The FM transition was manifested by a relatively smooth and gentle rise in the signal at low temperatures, and the amplitude of the transition decreased with increasing pressure. Above 7.4 GPa, no magnetic transition was observable. Also, as in the case of Gd, again we saw none of the additional peaks observed by McWhan and Stevens in their Dy susceptibility experiments.

D. Holmium

Holmium has both an AFM (basal-plane spiral structure) and a FM transition at low temperatures, with a T_N=133 K and a T_C=20 K. The latter transition was unfortunately near the lower temperature limit of our cryostat, so we were not able to accurately track its pressure dependence. Some high-pressure spectra are shown in Fig. 5. No magnetic transition was observable above 10.9 GPa.

E. Erbium

Erbium appeared to exhibit more interesting behavior than the previous elements discussed above. At zero pressure it has an AFM transition (c-axis sinusoidal) at T_N=80 K,

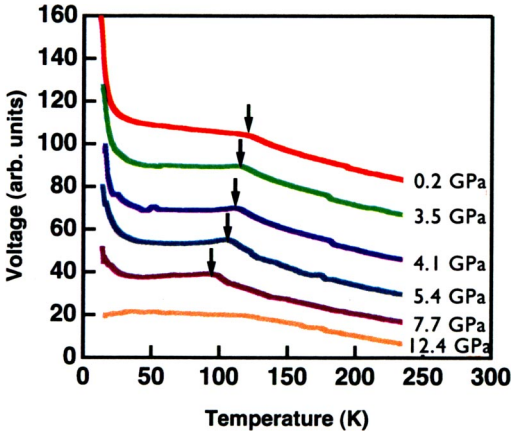

FIG. 5. (Color online) Magnetic susceptibility signal voltage versus temperature taken at various pressures for a holmium sample. The arrows show the location of the AFM transition.

followed by a FM transition at T_C=32 K. Under high pressures, T_N monotonically decreased at a roughly constant rate, while T_C remained relatively constant at ≈30 K for pressures up to about 10 GPa (Fig. 6). In addition, the amplitude of the peak at the Néel transition increased with increasing pressure, eventually becoming as large as the peak at the Curie temperature (see Fig. 7). Above approximately 13 GPa, the two peaks were indistinguishable, and we were not able to determine if this signified a transition to a FM or AFM phase. The magnetic transition signals then became weaker, eventually disappearing at pressures above 18.5 GPa.

F. Thulium

Like erbium, thulium also first ordered with a *c*-axis sinusoidal AFM phase (T_N=56 K) followed by a modulated FM phase at T_C=25 K. While we were clearly able to detect a sharp AFM transition, the FM transition was at the lower limit of our cryostat (see Fig. 8), and no upturn in the susceptibility was detected for P≳6.8 GPa, so it was not possible to track its pressure dependence. The Néel temperature was found to remain relatively constant at about 57 K up to about 4 GPa. It then decreased at a rate of dT_N/dP=−1.0 K/GPa until about 12 GPa. The shape of this peak then changed to a very broad voltage signal, which had a closer resemblence to the FM peak found in Dy than to the sharp AFM peak detected for Tm at lower pressures. In addition, this peak dropped off at a much faster rate of −8.4 K/GPa.

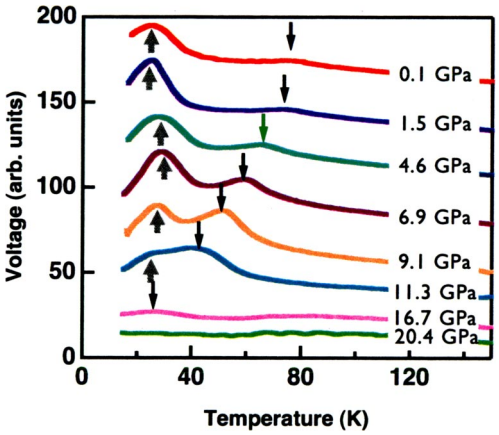

FIG. 6. (Color online) Magnetic susceptibility signal voltage versus temperature taken at various pressures for an erbium sample. The arrows pointing up show the location of the FM transition, and the downward arrows show the location of the AFM transition.

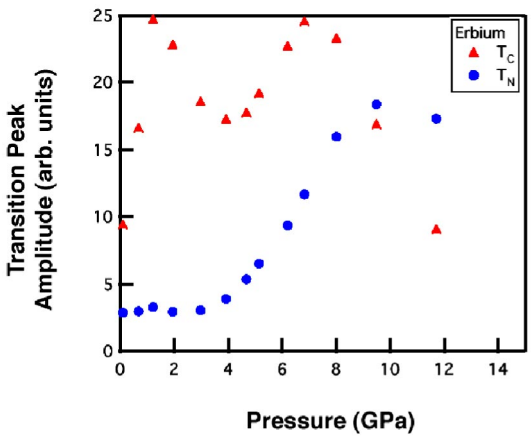

FIG. 7. (Color online) Amplitudes of the T_N and T_C peaks of erbium as a function of pressure. The amplitudes were obtained by least-squares, fitting the erbium magnetic susceptibility data shown in Fig. 6 to a double-Gaussian function.

IV. DISCUSSION

All of the above results are listed in Table I, in addition to many previous results from other researchers for comparison. The systematic trend observed for the heavy lanthanide elements Gd–Tm is for the magnetic ordering transitions to monotonically decrease with increasing pressure and then to disappear at a pressure ranging from about 5.5 GPa for Gd, to about 18.2 GPa for Er. The sensitivity limit of our current magnetic susceptibility technique is estimated to be around 10^{-2} emu/cm^3 for a 75 μm diameter sample. Our observa-

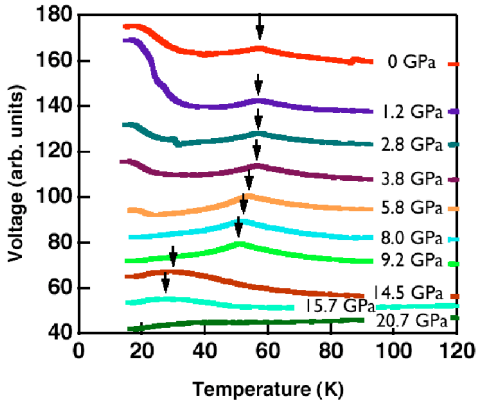

FIG. 8. (Color online) Magnetic susceptibility signal voltage versus temperature taken at various pressures for a thulium sample. The arrows show the location of the AFM transition.

TABLE II. Values used for $T(P=0)$, P_{crit} and $(-dT_{crit}/dP)/\{(g-1)^2J(J+1)\}$, where T_{crit} is the FM Curie temperature for Gd and Tb, and the AFM Néel temperature for Dy–Tm. For Er and Tm, the behavior of the voltage peak changes form at P_{crit}, but a magnetic phase persists up to the value given in parentheses.

Element	$(g-1)^2J(J+1)$	$T(P=0)$ (K)	P_{crit} (GPa)	$\frac{-dT_{crit}/dP)}{(g-1)^2J(J+1)}$ (K/GPa)
Gd	15.75	295	5.6	0.92
Tb	10.5	240	6.3	1.0
Dy	7.08	179	7.7	0.95
Ho	4.50	132	9.2	1.1
Er	2.55	79	9 (18.5)	1.2
Tm	1.17	60	12 (17)	0.88

tions are therefore limited by this sensitivity, so that when we discuss the disappearance of a magnetic transition, we mean that no signal is observable with our technique. Since AFM transitions can have signals much smaller than this, it is entirely possible that some type of AFM ordering with a very small signature persists in these elements to even higher pressures than reported here. Further work to improve the sensitivity of the magnetic susceptibility technique will be needed in order to explore this possibility.

The disappearance of magnetic ordering cannot be related to the delocalization of the *f* electrons and the vanishing of the individual atomic magnetic moments, since the pressures reported here are well below the reported or expected *f* electron delocalization pressures. For instance, the delocalization pressure of Gd has been reported to be about 60 GPa,[20] whereas its magnetic transition signal vanishes above only 5.6 GPa.

All six of the heavy lanthanides studied here stabilize in the hexagonal closed-packed (hcp) structure at room temperature and zero pressure. However, under pressure a number of structural phase transitions have been observed, mostly to other closed-packed structures such as the Sm-type, the double-hexagonal closed-packed (dhcp), and the face-centered-cubic (fcc) structures at even higher pressures. Unfortunately, the positions of these structural transitions at low temperatures are presently unknown. However, if we assume that the structural transition pressures at low temperatures remain approximately the same as their room-temperature values, there appears to be a case for arguing that the disappearance of the magnetic transition signals at high pressures is related to the onset of the dhcp phase. For example, the room-temperature dhcp phase transition in Gd is at 6 GPa,[20] and we detect a magnetic phase up to 5.6 GPa (see Fig. 9). Tb, Dy, and Ho also have a transition to a dhcp phase (6, 9, and 13 GPa, respectively[21]) near where we no longer observe a magnetic phase (see Table II). However, erbium and thulium do not fit in with this picture. A magnetic phase in Er persists to significantly higher pressures (disappearing at 18.5 GPa) than the room-temperature dhcp transition [13 GPa (Ref. 21)]. On the other hand, the magnetic phase in Tm disappears at a much lower pressure (17 GPa)

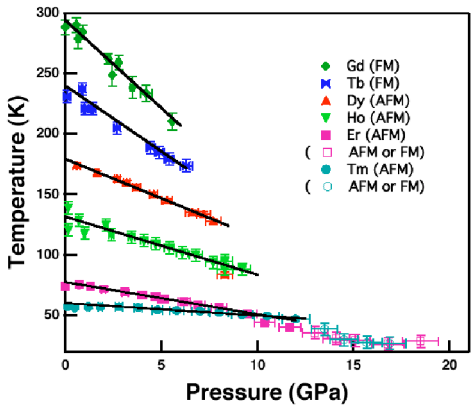

FIG. 9. (Color online) Magnetic ordering transition temperatures of Gd, Tb, Dy, Ho, Er, and Tm as functions of pressure.

than the onset of the room-temperature dhcp phase [30 GPa (Ref. 21)]. Further research to map out the structural phase diagrams of these elements at high pressures and low temperatures will be needed in order to shed more light on this issue.

The erbium susceptibility data appear to be particularly interesting. At low pressure, the magnitude of its T_N peak is much smaller than that of its T_C peak, as expected. However, with increasing pressure the magnitude of the T_N peak greatly increases by about a factor of 6, eventually becoming as large as the T_C peak at a pressure of about 9 GPa (see Figs. 6 and 7), and the two discernible peaks merge into one at about 12 GPa. This behavior suggests that the nature of the magnetic ordering at the T_N transition may be changing, with increasing pressure, from one having an AFM character to some sort of FM ordering with a nonzero net magnetization and, hence, a much larger ac-susceptibility response. This behavior is not seen in the AFM transitions of Dy, Ho, or Tm, which have AFM peaks that remain small with increasing pressure (Figs. 4, 5, and 8).

Although, for Tm, the amplitude of the peak at T_N does not increase with pressure, the pressure dependence of T_N is found to be more complex than that of the previous rare earths. Initially the Néel temperature remains fairly constant up to about 4 GPa, followed by a linear decrease up to about 12 GPa. At higher pressures, the behavior of the voltage at the magnetic transition changes from a sharp to a broad peak. In addition, the ordering temperature drops at a much faster rate, and the magnetic phase disappears below 20 K at about 17 GPa (see Fig. 9).

Both erbium and thulium exhibit "*c*-axis sinusoidal" AFM ordering, which means the magnetic moments are aligned parallel to the *c* axis with moment amplitudes that are sinusoidally modulated as a function of the *c*-axis position. On the other hand, the AFM order shown by dysprosium and holmium is a "basal-plane spiral" structure, in which the magnetic moment lies in the basal plane of the hexagonal structure and rotates around the *c* axis as a function of the *c* axis position. The difference between the ordering within the FM phases of erbium and thulium is that the moments in erbium have a helical structure which rotates about the *c* axis. The moments of thulium, on the other hand, are ori-

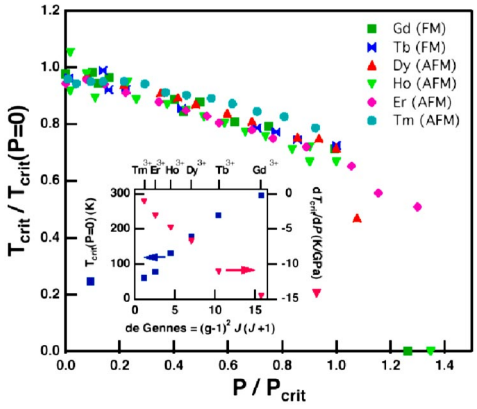

FIG. 10. (Color online) Magnetic ordering transition temperatures of Gd–Tm normalized to the ambient pressure transition as a function of pressure normalized to the critical pressure (see Table II). Inset shows the ambient pressure magneticordering transition temperature (left-hand side) and pressure derivative (right-hand side) vs the de Gennes factor.

ented parallel to the c axis, but are modulated so that four spins are aligned up, and the next three are down. Based on the magnetic susceptibility behavior observed here, it appears that these complex alignments for erbium and thulium become even more convoluted as the pressure is increased.

The coupling of the localized $4f$ electrons of the heavy rare-earth elements is through the RKKY interaction. This indirect interaction can be expressed as a Heisenberg Hamiltonian, $H_{ij}=-2\mathcal{J}_{ij}\mathbf{S}_i\cdot\mathbf{S}_j$, where $\mathcal{J}_{ij}$ is the exchange constant, and $\mathbf{S}_i$ is the localized spin at the ith ion. Due to spin-orbit effects, only the total angular momentums, $\mathbf{J}_i$ and not the $\mathbf{S}_i$, are constants of motion. The Wigner-Eckart theorem may be used to replace the spins by $\mathbf{S}_i=(g_J-1)\mathbf{J}_i$, where g_J is the Landé g factor. The transition temperatures θ_p within the Weiss molecular field theory are then expected at[1]

$$k_B\theta_p = 2\pi z A_0^2\{(g_J-1)^2 J(J+1)\}N(E_F)\sum_{\mathbf{R}_i\neq\mathbf{R}_j}\phi(2k_F|\mathbf{R}_i-\mathbf{R}_j|), \quad (1)$$

in which there are z conduction electrons per atomic volume, A_0 is the first-order coupling between the localized spins and the conduction electrons, $N(E_F)$ is the density of states at the Fermi level, k_F is the Fermi wave number, $\mathbf{R}_i$ is the lattice site of the ith localized spin, and $\phi(x)=[\sin(x)-x\cos(x)]/x^4$ is an oscillatory function due to the wave-number-dependent susceptibility.

At ambient pressure, Eq. (1) leads to the well-known prediction that the magnetic transition temperatures for the lanthanides should be roughly proportional to the term in brackets, $(g_J-1)^2J(J+1)$, which is known as the de Gennes factor. The inset to Fig. 10, which plots the highest transition temperature (left axis) vs the de Gennes factor, shows that this is in fact the case.

Predicting the pressure dependencies of the transition temperatures is more difficult, but here again, Eq. (1) provides some insights into the expected pressure behavior. First, note that for all of the elements studied here, the maximum pressures are all below the f electron delocalization pressures, so that both J and the de Gennes factor are constant for each element. One may then argue that to the first approximation, $|\mathbf{R}_i-\mathbf{R}_j|\sim a$, where a is the characteristic interatomic distance, and $k_F\sim 1/a$, so that their product has a rather weak pressure dependence, and the sum, $\Sigma\phi(2k_F|\mathbf{R}_i-\mathbf{R}_j|)$ will be fairly pressure independent. The remaining term in Eq. (1) is the density of states, $N(E_F)$. Considering the pressure effects on a simple tight-binding model as the pressure is increased, the atoms will move closer together, which will increase the bandwidth, thereby lowering the effective electron mass. Because the density of states at the Fermi level is proportional to the effective electron mass, increasing the pressure will result in reducing $N(E_F)$. Tokita *et al.*[13] have in fact suggested that, for Gd, the pressure dependence of the Curie temperature comes from a lowering of the conduction band, which decreases $N(E_F)$.

Therefore, the pressure dependence of Eq. (1) will be dominated by changes in the density of states. The inset to Fig. 10 shows the pressure derivative of the high-temperature magnetic phase, labeled dT_{crit}/dP (right axis), plotted against the de Gennes factor. The linear relationship shows that the heavy rare-earth elements remain RKKY magnets under pressure. In addition, as Table II shows, dT_{crit}/dP can be normalized by the de Gennes factor, and all of the heavy rare-earth elements have a fairly constant value. This shows that the density of states at the Fermi level, which is the dominant pressure-dependant factor of the RKKY interaction, has similar pressure dependence for all the heavy rare-earth elements.

Furthermore, we find that by properly scaling all of our transition temperatures and pressures, the data can be presented in the form of the universal plot shown in Fig. 10. In this plot, the highest transition temperatures have been normalized to their ambient pressure values, and the pressures have been normalized to P_{crit}, at which we no longer see a magnetic signal. We note that the pressures P_{crit} are somewhat subjective in the sense that they depend on the measurement sensitivity of our apparatus and the magnetic ordering which may persist to higher pressures. For Gd–Ho, any magnetic ordering at higher pressures is undetectable with our technique, but for Er and Tm, we have used the pressure where the magnetic ordering changes its character. For Er, we have used the pressure where the Néel and Curie transition peaks have about the same amplitude. For Tm, $P_{crit}=12$ GPa, above which the magnetic ordering behaves in a different manner. The correlations shown in Table II and Fig. 10 also neglect crystal-field effects, so the agreement may be only qualitative. Nonetheless, we empirically find that this scaling results in a consistent, universal description of the pressure dependencies of the highest transition temperatures.

The data shown in Fig. 10 indicate a strong similarity in the way that pressure affects the magnetic phases of the heavy rare-earth elements. Deviations from this universal curve indicate changes in the magnetic ordering. Two examples of this are Er and Tm, which have magnetic phases above $P/P_{crit}>1$. As was noted earlier, as the pressure is increased through this high-pressure region, the appearance of the voltage signal at the magnetic ordering temperature

takes on a new shape. It is not possible with our technique to determine if these high pressure phases continue to be AFM, or if they change to a FM ordering. There is also the possibility of changes in the crystalline structure which would have a large affect on the magnetic ordering. Another possibility is that the density of states at the Fermi level transforms. This behavior, though, could be a second-order effect driven by structural changes, for example. Further research will be needed to investigate these phases, for example, the field-dependent ac-magnetic susceptibility in which higher-order harmonics are measured, which would be nonzero in a FM phase due to nonlinear magnetization versus field dependence as the FM material approaches magnetic saturation.

V. CONCLUSION

We have measured the magnetic ordering transition temperatures of the heavy lanthanides Gd, Tb, Dy, Ho, Er, and Tm as functions of pressure using ac-magnetic susceptibility. The magnetic transition temperatures tend to monotonically decrease with increasing pressure. Additionally, the amplitudes of the magnetic transition signals for Gd–Ho and Tm diminish as the pressure is increased, while Er is found to have a complex pressure dependence for the amplitudes of both T_N and T_C. If the transition temperatures are normalized to their ambient pressure values, and the pressures are normalized to the values at which the transitions disappear, then all of the data line up on a single-phase diagram. Finally, for each element, the rate of change of its magnetic transition temperature with pressure scales very well with its de Gennes factor. Both of these behaviors can be attributed to the pressure dependence of the density of states at the Fermi level.

ACKNOWLEDGMENTS

We would like to thank Reed Patterson, Chantel Aracne, Dave Ruddle, and Steve Falabella for their help in the experiments. We also thank Ron Lee, L.T. Wiley, B.T. Goodwin, and J. Akella for their support of this work. This work was performed under the auspices of the U.S. Department of Energy by the University of California, Lawrence Livermore National Laboratory, under Contract No. W-7405-Eng-48.

*Electronic address: djackson@mailaps.org

[1] K. N. R. Taylor and M. I. Darby, *Physics of Rare Earth Solids* (Chapman and Hall Ltd, London, 1972).
[2] R. J. Elliott, *Magnetism, A Treatise on Modern Theory and Materials* (Academic Press, New York, 1965).
[3] L. Patrick, Phys. Rev. **93**, 384 (1954).
[4] L. B. Robinson, F. Milstein, and A. Jayaraman, Phys. Rev. **134**, A187 (1964).
[5] L. B. Robinson, S.-I. Tan, and K. F. Sterrett, Phys. Rev. **141**, 548 (1966).
[6] D. McWhan and A. Stevens, Phys. Rev. **139**, A682 (1965).
[7] D. McWhan and A. Stevens, Phys. Rev. **154**, 438 (1967).
[8] F. Milstein and L. B. Robinson, Phys. Rev. **159**, 466 (1967).
[9] J. E. Milton and T. A. Scott, Phys. Rev. **160**, 387 (1967).
[10] A. R. Wazzan, R. S. Vitt, and L. B. Robinson, Phys. Rev. **159**, 400 (1967).
[11] H. Bartholin and D. Bloch, J. Phys. Chem. Solids **29**, 1063 (1968).
[12] T. Iwamoto, M. Mito, M. Hidaka, T. Kawae, and K. Takeda, Physica B **329–333**, 667 (2003).
[13] M. Tokita, K. Zenmyo, H. Kubo, K. Takeda, M. Mito, and T. Iwamoto, J. Magn. Magn. Mater. **272–276**, 593 (2004).
[14] H. Mao, P. Bell, J. W. Shaner, and D. Steinberg, J. Appl. Phys. **49**, 3276 (1978).
[15] D. Ragan, R. Gustavsen, and D. Schiferl, J. Appl. Phys. **72**, 5539 (1992).
[16] W. Vos and J. Schouten, J. Appl. Phys. **69**, 6744 (1991).
[17] D. Jackson, C. Aracne-Ruddle, V. Malba, S. Weir, S. Catledge, and Y. Vohra, Rev. Sci. Instrum. **74**, 2467 (2003).
[18] S. Catledge, Y. Vohra, S. Weir, and J. Akella, J. Phys.: Condens. Matter **9**, 67 (1997).
[19] S. Weir, J. Akella, C. Aracne-Ruddle, Y. Vohra, and S. A. Catledge, Appl. Phys. Lett. **77**, 3400 (2000).
[20] H. Hua, Y. Vohra, J. Akella, S. Weir, R. Ahuja, and B. Johansson, Rev. High Pressure Sci. Technol. **73**, 233 (1998).
[21] D. A. Young, *Phase Diagrams of the Elements* (University of California Press, Berkeley, CA, 1991), and references therein.